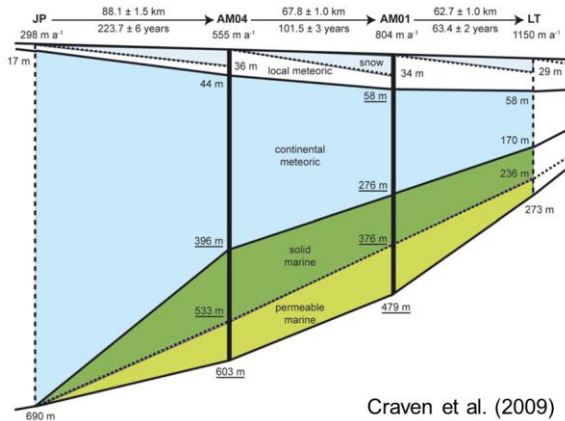


**A SEA ICE APPROACH TO MODELING BULK DENSITY VARIATIONS CAUSED BY NON-ICE IMPURITIES.** N. S. Wolfenbarger<sup>1</sup>, K. M. Soderlund<sup>1</sup>, and D. D. Blankenship<sup>1</sup>, <sup>1</sup>Institute for Geophysics, University of Texas at Austin, J.J. Pickle Research Campus, Bldg. 196; 10100 Burnet Road (R2200), Austin, TX 78758 (nwolfenb@utexas.edu),

**Introduction:** The bulk thermophysical properties of ice are of critical importance to governing dynamic processes responsible for generating the features we observe at the surfaces of icy worlds across the solar system (e.g., fracture, diapirism, convection) [1]. The presence of non-ice impurities alters these bulk thermophysical properties relative to that of pure ice. Here, we specifically focus on how bulk ice density as a function of temperature is influenced by the presence of salts.

For terrestrial sea ice, the bulk ice density can be represented using the density and volume fraction of each phase (i.e., the volume fraction of air, brine, pure ice, and solid salts) [2]. We first examine how variations in bulk ice salinity resulting from different mechanisms of freezing (i.e., frazil vs. congelation, see [3]) generate different bulk ice density profiles and column-averaged bulk ice densities. We apply our model to two Antarctic ice shelves (Amery Ice Shelf and Ross Ice Shelf), where ice cores were able to sample the accreted ice layer [4,5]. We then extend our model to consider impurity compositions beyond Earth, focusing on Jupiter’s ice-covered moon Europa.



**Figure 1.** Illustration of the thickness and characteristics of marine ice layers, formed through the accumulation and consolidation of frazil ice crystals, beneath Amery Ice Shelf, East Antarctica from [4].

**Methods:** We adopt the approach of [6] and represent the phase behavior (i.e., the change in brine and precipitate properties as a function of temperature) for a given solution composition using piecewise polynomial functions of temperature, derived from the

output of aqueous geochemistry software. The so-called phase behavior functions are defined as

$$F_1(T) = \rho_b(T)S_b(T)(1 + k(T))$$

where  $\rho_b$  is the brine density ( $\text{g/cm}^3$ ),  $S_b$  is the brine salinity (ppt), and  $k$  is the ratio of mass of salts in the form of solid salts to the mass of salt in the brine, and

$$F_2(T) = (1 + C(T)) \frac{\rho_b(T)}{\rho_i(T)} - \frac{C(T)\rho_b(T)}{\rho_{ss}(T)} - 1$$

where  $C$  is the ratio of mass of solid salts to the mass of brine,  $\rho_b$  is the brine density ( $\text{g/cm}^3$ ),  $\rho_i$  is the pure ice density ( $\text{g/cm}^3$ ), and  $\rho_{ss}$  is the density of solid salts ( $\text{g/cm}^3$ ). For application to sea ice, we use phase behavior functions defined in [6]. Unlike in [6] we use these phase behavior functions to directly model the bulk ice density, as opposed to modeling the volume fraction of each phase. We follow the approach of [2] and represent the bulk ice density as

$$\rho(T) = \left(1 - \frac{V_a}{V}\right) \frac{\rho_i(T)S}{F_1(T) - \rho_i(T)SF_2(T)}$$

where  $\frac{V_a}{V}$  represents the volume fraction of gas (air in the case of sea ice) and  $S$  is the bulk ice salinity. The density of pure ice is modeled using the equations adopted by the International Association for the Properties of Water and Steam (IAPWS), originally published in [7]. Although  $\frac{V_a}{V}$  is represented as constant here, this parameter is governed by overburden pressure, temperature, and/or melt drainage. In newly formed sea ice or ice forming beneath ice shelves  $\frac{V_a}{V}$  can be assumed to be zero; however, for brine injected firm this assumption is no longer valid [8]. For planetary applications,  $\frac{V_a}{V}$  is critically important within the regolith, above the pore-close off depth, and likely negligible below this depth [9].

**Results and Discussion:** We have applied the approach of [6] to generate a parameter sweep of brine volume fraction (Fig. 2), salt volume fraction (Fig. 3), and bulk ice density (Fig. 4) for temperatures and bulk ice salinities relevant to sea ice and ice forming beneath terrestrial ice shelves. The minimum temperature we

consider is the freezing temperature for terrestrial seawater (approximately  $-2\text{ }^{\circ}\text{C}$ ). We note that sea ice can be stable at temperatures higher than  $-2\text{ }^{\circ}\text{C}$  although these would represent conditions consistent with the onset of melting.

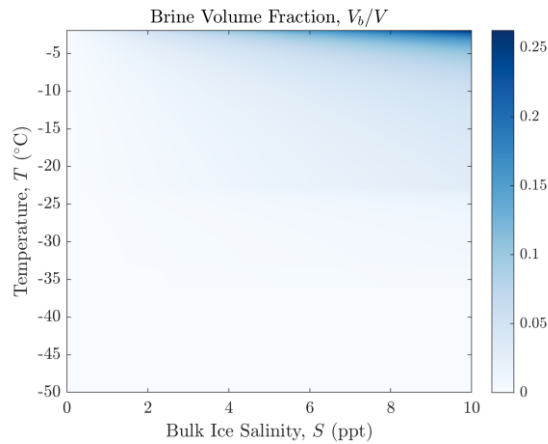


**Figure 2.** Brine volume fraction for terrestrial sea ice as a function of temperature and bulk ice salinity.

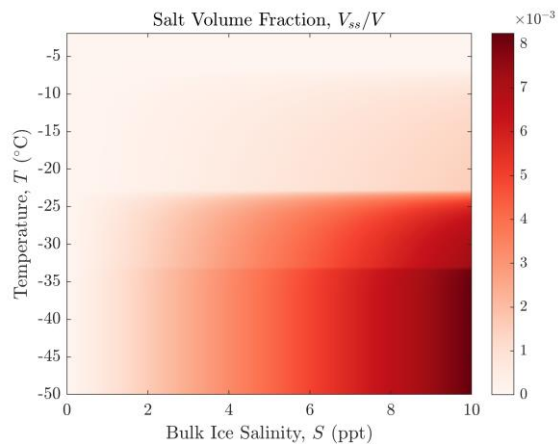


**Figure 3.** Salt volume fraction for terrestrial sea ice as a function of temperature and bulk ice salinity.

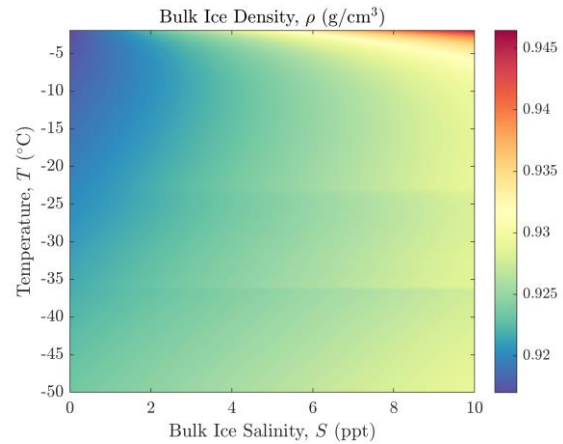


**Figure 4.** Bulk ice density for terrestrial sea ice as a function of temperature and bulk ice salinity. The horizontal features visible in the plot reflect the effect hydrohalite precipitation at  $-22.9\text{ }^{\circ}\text{C}$  and the transition below the eutectic temperature at  $-36.2\text{ }^{\circ}\text{C}$ .

It is evident from Figure 4 that although the non-ice volume fraction is low (Fig. 2 and 3), it influences the bulk ice density both above and below the eutectic temperature. We will apply this model to our two terrestrial analog sites to quantify the density profile and the column-averaged density associated with the accreted ice layer at these sites. We will then apply this model to Europa, quantifying density variations in the ice shell resulting from heterogeneous accretion at the ice-ocean interface [3] and the solidification of brine reservoirs [10,11].

**References:** [1] Soderlund, K. M. et al. (2020) *Space Sci Rev*, 216, 1–57. [2] Cox G. F. N. and Weeks W. F. (1983) *J. Glaciol.*, 29, 306–316. [3] Wolfenbarger, N. S. et al. (2022) *Astrobiology*, 22, 937–961. [4] Craven, M. et al. (2009) *J. Glaciol.*, 55, 717–728. [5] Zotikov, I. A. et al. (1980) *Science*, 207, 1463–1465. [6] Wolfenbarger, N. S. et al. (2022) *J. Geophys. Res. Planets*, 127, e2022JE007305. [7] Feistel, R. and Wagner, W. (2006) *J. Phys. Chem. Ref. Data*, 35, 1021–1047. [8] Grima, C. et al. (2016) *Geophys. Res. Lett.*, 43, 7011–7018. [9] Aglyamov, Y. et al. (2017) *Icarus*, 281, 334–337. [10] Chivers, C. et al. (2021) *J. Geophys. Res. Planets*, 126, e2020JE006692. [11] Lesage, E. et al. (2022) *Planet. Sci. J.*, 3, 170.